13th World Conference on Earthquake Engineering
Vancouver, B.C., Canada
August 1-6, 2004
Paper No. 3495

# RESPONSE EVALUATION OF AMOLANAS BRIDGE USING SEISMIC, WIND AND TEMPERATURE RECORDS

**Cesar BELTRAN[1], Maria MORONI[2], Mauricio SARRAZIN[3]**

## SUMMARY

The Amolanas bridge, located 309 Km north of Santiago, Chile, presents several outstanding features, like a 268 m steel continuous box girder, a 100 m tall pier, friction bearings on two piers and at abutments and two dampers at each abutment in the longitudinal direction. Being located in an active seismic zone, it has been advisable to monitor its behavior with some permanent instrumentation.

A network consisting on 12 accelerometers was installed the year 2000. Five moderate earthquake have been registered since then. Later, a second network consisting on an anemometer and displacement and temperature sensors has been installed allowing to monitor the dampers and friction bearings performance to wind and temperature actions and to detect, if any, permanent deformations. Previous to these installations, ambient vibration measurements were performed.

This paper presents data from field measurements and numerical results from theoretical modeling. A finite element model was developed aimed to reproduce the motions obtained at the site. Time history analysis as well as frequency analysis was used to compare experimental and calculated response. The friction coefficient, modal damping and concrete modulus of elasticity were used as calibration parameters. These values depend on the level of vibration, thus for larger earthquakes new calibrations will be needed since the bridge behaviour is highly non-linear.

Wind and temperature effects on the bridge structure is also analysed. The combined effect of this two actions is presented, concluding that for design wind and normal temperature variation the structure ends up with a permanent displacement of the order of 40 mm.

[1] Graduate student, Department of Civil Engineering, University of Chile
[2] Associate Professor, Department of Civil Engineering, University of Chile
[3] Professor, Department of Civil Engineering, University of Chile, sarrazin@ing.uchile.cl

## INTRODUCTION

The Amolanas bridge, which uses a combination of sliding bearings and viscous dampers, is located at 309 Km to the North of Santiago, in the North – South Pan-American Highway. The bridge is described in Sarrazin et al.[1]. In summary, it consists of a continuous steel box girder 268 m. long, with cantilever structures at both sides. This girder stands on sliding supports in the longitudinal direction, with the exception of the connection at the tallest pier, which is fixed in all directions. As shown in figure 1, there are 3 reinforced concrete piers with heights, from South to

Figure 1. Overall view of the Amolanas Bridge.

North, of 26.3, 53.1 and 99.6 m, respectively. Two non-linear viscous dampers are located at each abutment as can be seen in figure 2. The piers are octagonal hollowed section. They stand on individual rectangular foundations supported on rock.

Figure 2. Dampers at North abutment.

In the transverse direction, the superstructure is quite rigid as compared with the lateral flexibility of the tallest piers. Although the shortest pier, C1, is relatively stiff, most of the horizontal seismic forces coming from the superstructure are transmitted to the abutments.

In the longitudinal direction, the seismic motion is limited in part by the friction pads and primarily by the viscous dampers at the abutments. The tallest pier is hinged at the top to the superstructure, which acts then as a support for the pier under horizontal forces. The other two piers interact with the superstructure through friction forces between Teflon pads and stainless steel plates. A friction coefficient equal to 0.025 was considered in the design phase, but it can vary between 0.01 and 0.03, according to the bearings supplier. The viscous dampers are non-linear, having the following velocity-force law: $F = 3000\ V^{0.15} \pm 15\%$, where $F$ is the transmitted force in [kN] and $V$ is the velocity in [m/s]. Forces are very small for low velocities and are almost constant for velocities larger than 0.2 m/sec; this allows thermal expansions with limited forces.

After construction, in 2000, the bridge was instrumented with a network of 12 digital accelerometers for continuous monitoring (Episensors, of Kinemetrics). Three of them are located on the "free field" while the remaining are distributed along the deck and at the abutments (figure 3). With this network, ambient vibration and five moderate earthquakes have been recorded. It has also been instrumented with a monitoring system to measure relative displacements at the sliding supports on the abutments and at piers 1 and 2; an anemometer to measure the velocity and direction of wind, and a network of temperature sensors at the steel box beam and at the superstructure's slab.

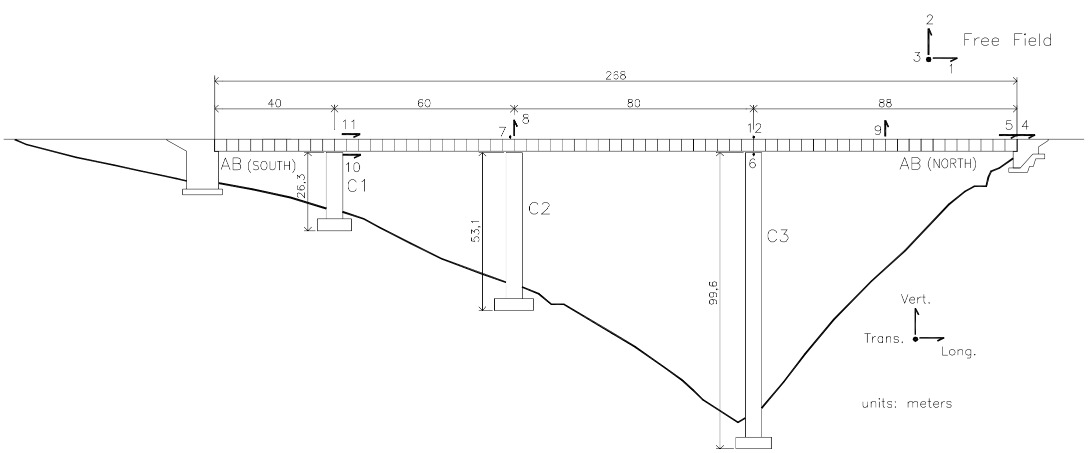


Figure 3. Accelerometers location.

The fundamental structural dynamic properties of the bridge have been studied using ambient vibration recorded by means of a portable temporary accelerometers network, and by the permanent instrumentation. The recorded vibration data are being processed aiming to identify the natural frequencies and modal shapes by means of standard time and frequency domain techniques. They include band-pass filters and power spectral and cross-spectral density functions analysis. The responses to these small vibrations are nearly linear, thus representing just a starting point for the understanding of the behavior of the bridge when subjected to real earthquakes for which the response is expected to be highly non-linear. A finite element linear elastic model capable of approaching the experimental modes of vibration was developed.

Finally, results obtained for wind, temperature and displacement recorded by the corresponding instruments are presented. This data is analyzed by means of a non-linear model that allows to predict displacements due to combined wind and temperature effect.

## MICROVIBRATION MEASUREMENTS

Ambient vibration data was initially recorded at the structure with a portable network and later with the permanent network. The portable network consists of six seismic velocity sensors (Ranger SS-1) with flat response between 1 and 100 Hz, connected to a single recording station. Typical recording time varied from 5 to 20 minutes and sampling rates from 100 to 200 Hz. Selection of the corresponding values depends on the energy of the predominant frequencies.

The natural frequencies and the modes of vibration were obtained from the power spectral density and the correlation functions between the different records. An approximation to the equivalent viscous damping was obtained by means of the bandwidth method, Tanaka [2]. Table I shows the

**Table I. Dynamic characteristics, Amolanas bridge**

Results obtained with accelerometers FBA-11

| Mode | Frequency [Hz] | Period [sec] | Damping [%] | Predominant direction |
|---|---|---|---|---|
| 1 | 0.68 | 1.46 | 4.40 | Transverse -Vertical |
| 2 | 1.32 | 0.76 | 1.60 | Longitudinal - Vertical |
| 3 | 1.66 | 0.60 | 1.64 | Transverse |
| 4 | 2.05 | 0.49 | 1.21 | Transverse –Vertical -Longitudinal |
| 5 | 2.95 | 0.34 | 1.01 | Longitudinal |

Results obtained with seismometers SS-1

| Mode | Frequency [Hz] | Period [sec] | Damping [%] | Predominant direction |
|---|---|---|---|---|
| 1 | 0.68 | 1.46 | 3.40 | Transverse |
| 2 | 1.34 | 0.75 | 1.46 | Longitudinal- Vertical |
| 3 | 1.71 | 0.59 | 1.61 | Transverse |
| 4 | 2.05 | 0.49 | 1.36 | Transverse-Vertical-Longitudinal |
| 5 | 2.95 | 0.34 | 1.03 | Longitudinal |

first five natural frequencies, periods and values of damping determined from the records of the accelerometers and from the seismometer data. It can be seen that the differences in the estimated natural frequencies from the two types of instruments is less than 3 %. However, the differences in the damping values are larger, particularly in the first mode where the accelerometer records provided a value of 4.4 % whereas the seismometers yielded 3.4 %.It is interesting to notice that in both cases the damping tends to decrease with increasing frequency although not in a uniform way. The damping in the first mode is estimated at between 3.4 and 4.4 % whereas in the fifth mode the values are 1.01 and 1.03 %.

## EARTHQUAKE RECORDS

The main characteristics of the five earthquakes recorded by the acceleration network are shown in Table II. Table III shows the ratio between peak accelerations recorded by the different sensors.

**Table II. Characteristics of seismic records, Amolanas bridge**

| Date | Depth km | Max. accel free field | Max. Accel bridge | Magnitude Richter |
|---|---|---|---|---|
| 23-12-2001 | 27.1 | 0.039 (T) | 0.022 (7) | 4.9 |
| 01-04-2002 | 67.0 | 0.029 (L) | 0.036 (9) | 6.2 |
| 23-05-2002 | 53.7 | 0.098 (L) | 0.067 (9) | 5.8 |
| 18-06-2002 | 52.2 | 0.104 (T) | 0.112 (9) | 6.3 |
| 20-06-2003 | 24.1 | 0.093 (L) | 0.090 (9) | 6.2 |

( ) indicates direction or sensor number

**Table III. Maximum peak acceleration ratios. Amolanas bridge**

| Date | 23-12-01 | 01-04-02 | 23-05-02 | 18-06-02 | 20-06-03 |
|---|---|---|---|---|---|
| Long North abutment/free field (a4/a1) | 1.45 | 1.41 | 0.87 | 1.68 | 1.43 |
| Long superst/abutment North (a5/a4) | 0.36 | 0.30 | 0.32 | 0.31 | 0.27 |
| Long superst/top pier 1 (a11/a10) | 0.30 | 0.46 | 0.80 | 0.35 | 0.86 |
| Long superst/superst North end (a11/a5) | 0.41 | 0.54 | 0.92 | 0.72 | 1.0 |
| C3, Trans superst/top pier (a12/a6) | 1.01 | 0.83 | 1.26 | 1.03 | 1.02 |
| C3, Trans superst/free field (a12/a3) | 0.48 | 0.63 | 0.54 | 0.54 | 0.80 |
| Vertical superst North span/free field (a9/a2) | 1.33 | 2.95 | 1.97 | 2.33 | 2.20 |
| C2, Vert Superst/free field (a8/a2) | 1.33 | 1.50 | 1.41 | 1.43 | 1.20 |

ai/aj refers to sensor numbers from fig. 3

The maximum peak accelerations in the longitudinal direction at the north abutment (sensor 4) are usually (except for one case) larger than on the free field. The longitudinal peak accelerations on the deck (sensors 5 and 11) are substantially smaller than those of the abutments and smaller than those on top of pier 1. The peak transverse accelerations on the deck are smaller than those in the free field (about half) but of the same order of those on top of pier 3. Important reductions are seen in the longitudinal direction while the contrary is observed in the vertical direction. Modal identification showed that the natural frequencies varied with and during each event and were slightly different from those obtained from ambient vibration measurements. There is a fundamental transverse mode at 0.63-0.66 Hz, and a fundamental longitudinal mode at 0.9-1.3 Hz. The maximum variation occurs in the longitudinal direction. Using again the bandwidth method, equivalent damping values were obtained; in Table IV they are compared with those calculated from the ambient vibrations measurements. It can be observed that for the first longitudinal frequency (the second natural frequency) there is a considerable increase in damping from 1.6 to

**Table IV. Damping in Amolanas Bridge**

| Frecuency Hz | Direction | Damping earthquakes | Damping ambient vibration |
|---|---|---|---|
| 0.63-0.66 | Transverse | 0.045 | 0.044 |
| 0.90-1.30 | Longitudinal | 0.041 | 0.016 |
| 1.21-1.28 | Vertical | 0.027 | 0.016 |
| 1.60-1.65 | Transverse | 0.018 | 0.016 |
| 2.01-2.08 | Trans-Vert | 0.014 | 0.012 |

4.1%.This can be explained by the energy dissipated by friction at the sliding bearings that gets mobilized with increasing vibration amplitudes.

Figure 4 shows the longitudinal accelerations recorded at four sensors on June 18$^{th}$ 2002 (sensor 1 in the free field, sensor 5 on the deck near the abutment, sensor 10 on top of pier 2 and sensor 11 at the same location but on top of the deck). The figure shows also the Fourier spectra of these motions. The motions recorded in the free field and on the abutment (sensor 4, not shown in the figure) had very similar frequency contents with somewhat reduced amplitudes in the Fourier spectrum for sensor 4. It can be seen that the motion in the free field has some large amplitudes in the range from 3.5 to 5 Hz with a peak of 120 at about 4.2 Hz. The motion of sensor 10 (notice the different scales) has a main peak with a value of about 42 at 4.5 Hz and smaller peaks around 1.2, 2, 3, 3.7 and 4 Hz. The longitudinal motions recorded on the deck exhibit a main peak at about 1.1 Hz (fundamental longitudinal frequency of the bridge for this earthquake level) with a value of about 17 near the abutment and slightly less over pier 2. There are additional peaks at 4 and 4.7 Hz with amplitudes of about 7 and 6 near the abutment and only 2 and 6 respectively over the pier. These figures illustrate clearly the effectiveness of the protection system in reducing the longitudinal accelerations, filtering out considerably the high frequency components of the earthquake while amplifying the very small components at the natural frequencies of the structure.

Displacements were obtained through double integration of the acceleration records with appropriate base line corrections; the largest ones occurred during the earthquake of 18/06/2002. They had values of 0.47 cm, 0.68 cm and 0.36 cm in the longitudinal (deck), transverse (pier 3) and vertical (north span) direction, respectively.

Figure 5 shows the longitudinal displacements of sensors 5 and 11, both on the deck, and sensor 10 on top of pier 1. It can be seen that the displacements of sensors 5 and 11 are almost identical indicating a rigid body motion of the deck in the longitudinal direction. It should be noticed that there is a permanent displacement. There were clear out of phase motions between the top of pier 1 and the deck and between the deck and the abutment. The largest relative longitudinal displacement at the sliding bearings was 0.41 cm at the north abutment.

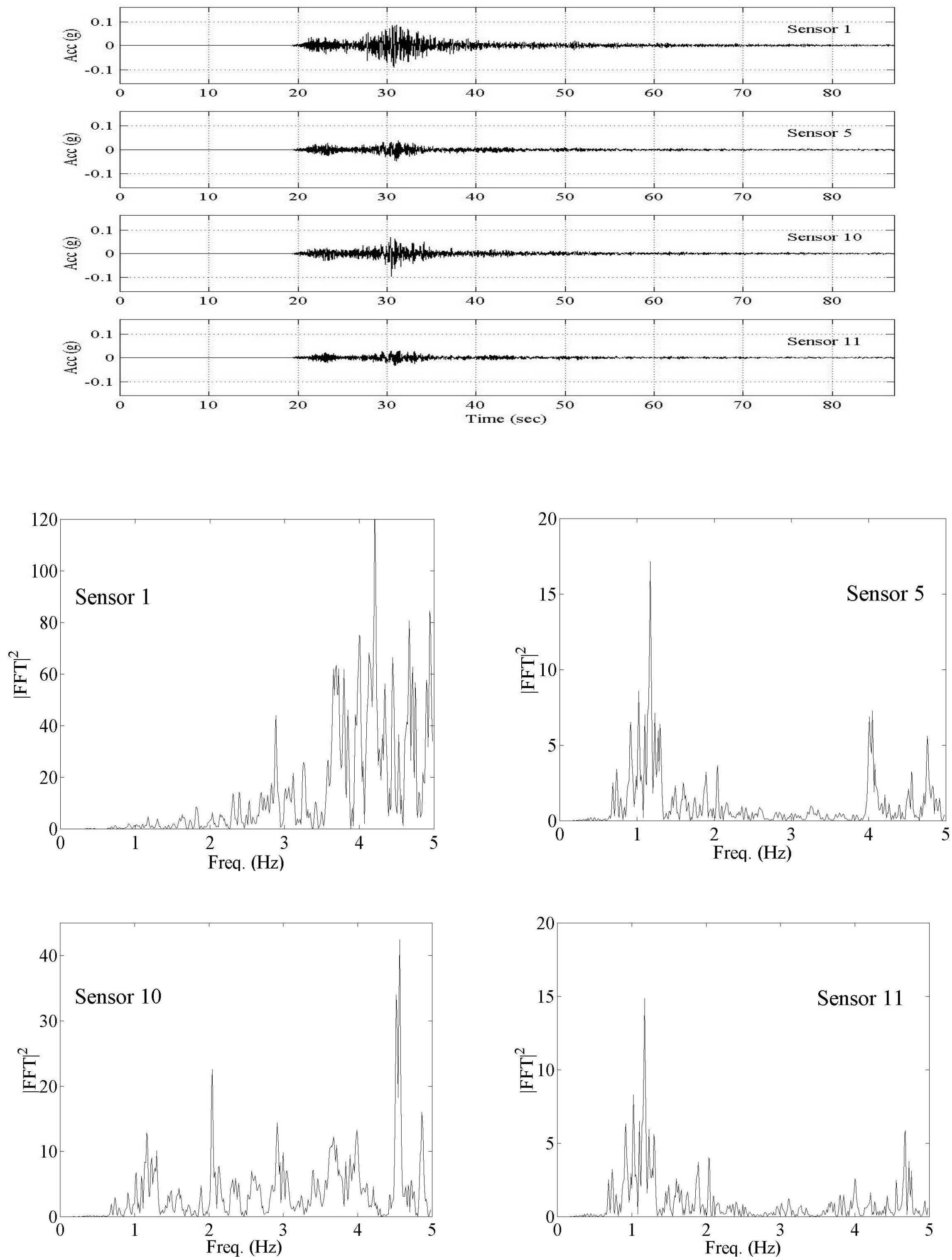


**Figure 4. Longitudinal acceleration records and squared Fourier Spectra, 18/06/02 earthquake**

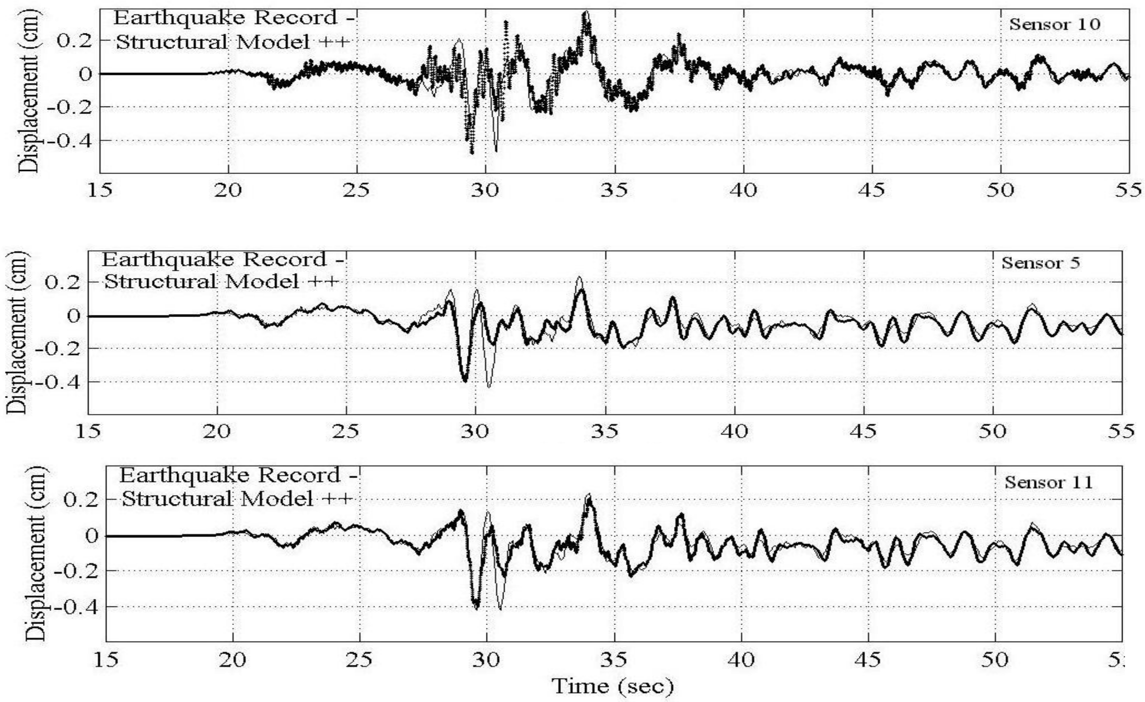


(a)

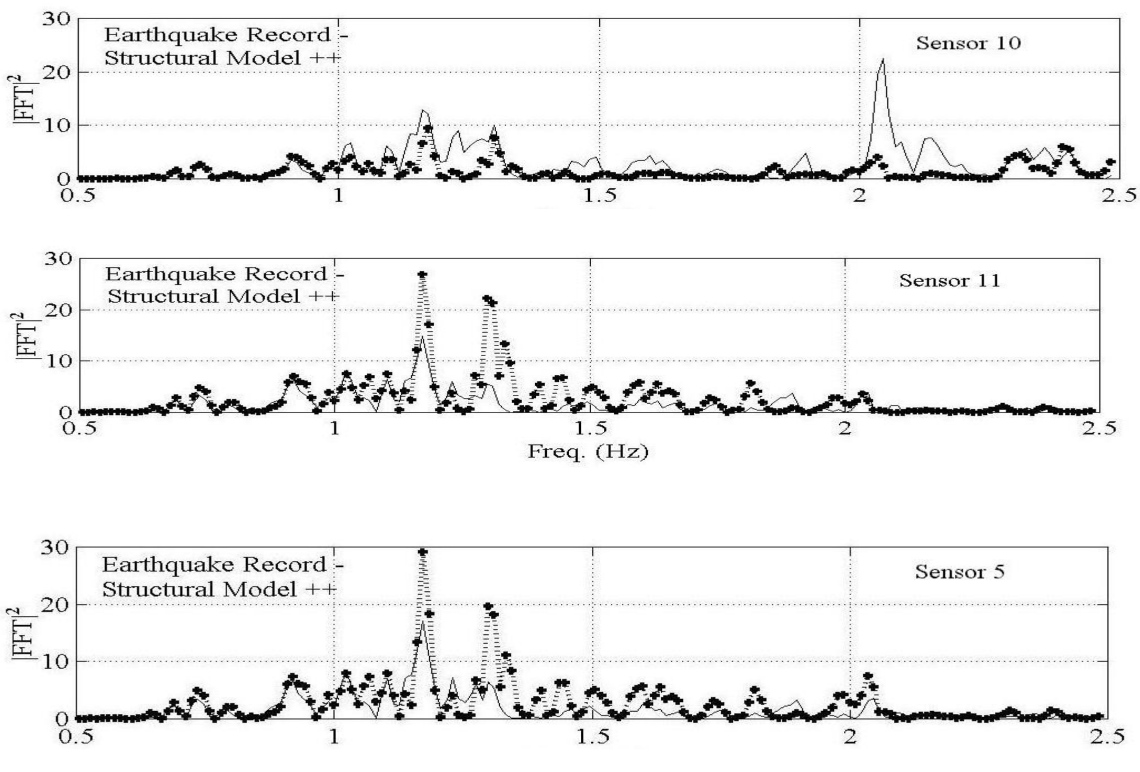


(b)

**Figure 5. Experimental and predicted results, June 18th, 2002 (a) longitudinal displacements; (b) FFT$^2$**

## STRUCTURAL MODEL

A linear model is appropriate to reproduce the results of the ambient vibration tests because their small amplitudes do not trigger the sliding supports, nor produce any effect at the viscous dampers. The first four natural frequencies computed with a linear finite element model that runs in SAP2000NL had values of 0.69, 1.36, 1.73, and 1.86 Hz (versus 0.68, 1.32, 1.66 and 2.05 obtained from the measurements). Friction bearings were represented by hinged bars and the dampers at the abutments were not included.

However, for large vibrations, as will be the case for the design earthquake, the system will be highly non linear and only a time history analysis should be appropriate. The finite element model was thus modified to simulate the seismic response. Friction bearings were represented by NLLINK elements. Considering that the foundation soil is hard rock for all piers and the abutments, the input motion was considered identical at the base of all of them and equal to the motion recorded in the free field, that is, at the bottom of an excavation 3 m deep located at a distance of 30 m to the north of the north abutment. The friction coefficient, modal damping and concrete modulus of elasticity were used as calibration parameters. Dampers were considered increasing the modal damping associated with the longitudinal modes, (10% for the 2$^{nd}$ mode). For the larger earthquakes the best fit in displacements occurred for a friction coefficient equal to 3.5%. The computed accelerations at the various sensors, the corresponding Fourier spectra and the displacements were in general in good agreement with the measurements although there were some clear discrepancies. Figure 5 shows the measured and calculated longitudinal displacements for the 18/06/2002 earthquake and their Fourier spectra. The time histories show some differences in the amplitudes of the peaks (notably around 30 sec) but overall the agreement is remarkably good. The discrepancies are more apparent in the amplitude Fourier spectra, notably around 2 Hz for sensor 10, but also in the 1.2 to 1.3 Hz region.

## WIND AND TEMPERATURE EFFECTS.

Since the bridge superstructure is resting on sliding bearings in the longitudinal direction, the only restoring force in that direction comes out from pier C3, which is quite flexible due to its slenderness. It could be expected, therefore, that for a combined action of wind and temperature changes, the bridge superstructure could slither after a number of cycles, thus ending up with a permanent displacement. This initial sliding could affect the performance of the viscous dampers if an earthquake were to happen. To investigate this possibility new equipment has been installed in the bridge to record in real time the following variables: wind velocity and direction, temperature distribution along and across the superstructure, and relative displacements at abutments and over piers C1 and C2. The equipment, consists of a Data Logger 300, an anemometer Young Instruments 05103VM, four relative displacement sensors, eight temperature sensors and two Solar Panel SP75 to provide energy.

### Wind effect.

The anemometer is installed between piers C1 and C2, below the main beam, and has been recording wind direction and velocity since September 27, 2003 Farias [3]. Table V contains a summary of the maximum velocities and their corresponding directions. The velocities recorded are quite low and do not produce any important effect on the bridge. Therefore AASHTO recommendation for maximum design wind velocity was used in a theoretical simulation. It was assumed that the wind velocity varies linearly from zero to the maximum value in 8 sec, then remains constant for 10 sec and finally returns to zero en 7 sec. The same cycle was repeated twice. A finite element model using SAP2000NL was carried out for three different values of friction coefficient, namely 1, 2 and 3 %. The sliding supports were modeled by means of NLLINK elements. Figures 6 and 7 contain the relative displacements and shear forces at the different supports for 1 and 3 % friction, respectively. These results show that the wind in the longitudinal direction, acting from South to North over the piers and the super-structure, could produce a permanent displacement of the super-structure of near 50 mm for a low friction coefficient (1 %) and 3 mm for a larger friction coefficient (3 %). Note that the bridge was designed using a friction coefficient of 2.5 %.

**Table V. Summary of maximum wind velocities**

| | Sep. | | Oct. | | Nov. | | Dec. | |
|---|---|---|---|---|---|---|---|---|
| | Vel | Dir | Vel | Dir | Vel | Dir | Vel | Dir |
| | [m/s] | [º] | [m/s] | [º] | [m/s] | [º] | [m/s] | [º] |
| Max | 8.8 | 301.3 | 11.7 | 303.2 | 10.3 | 71.5 | 15.5 | 289.8 |
| Min | 0.5 | 26.4 | 0.5 | 18.4 | 0.5 | 4.6 | 0.5 | 25.2 |
| Average | 2.8 | 240.7 | 3.8 | 271.1 | 2.0 | 181.8 | 4.7 | 293.4 |

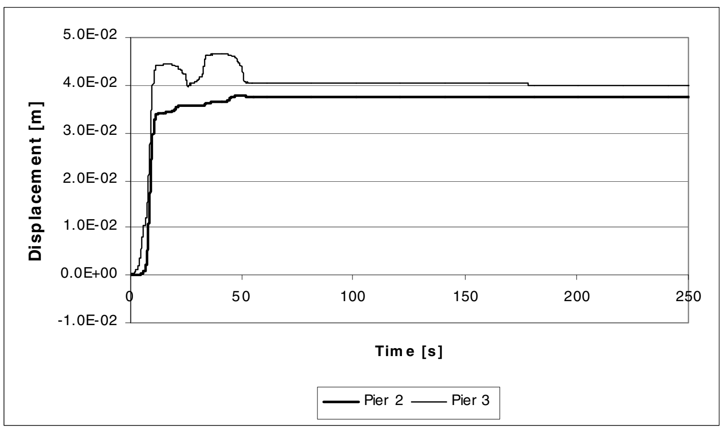


Coefficient of friction = 0.01

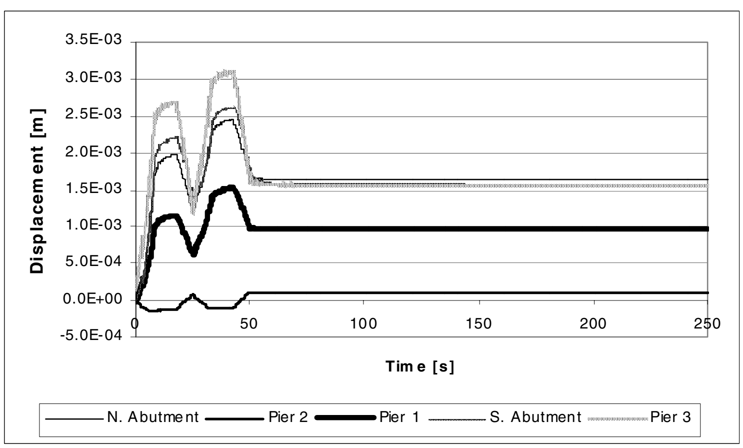


Coefficient of friction = 0.03

**Figure 6. Displacements due to wind.**

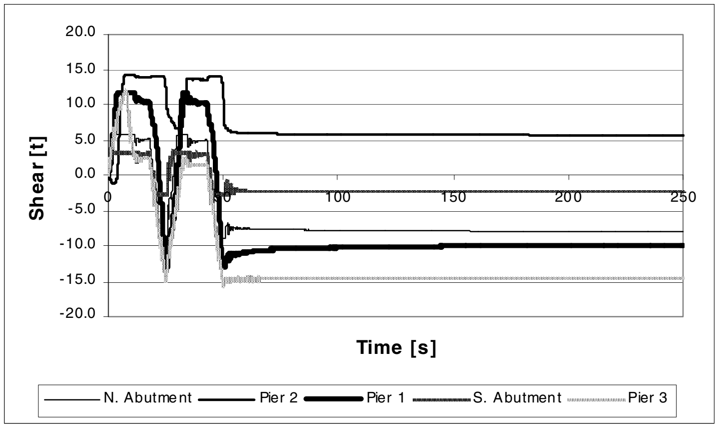


Coefficient of friction = 0.01

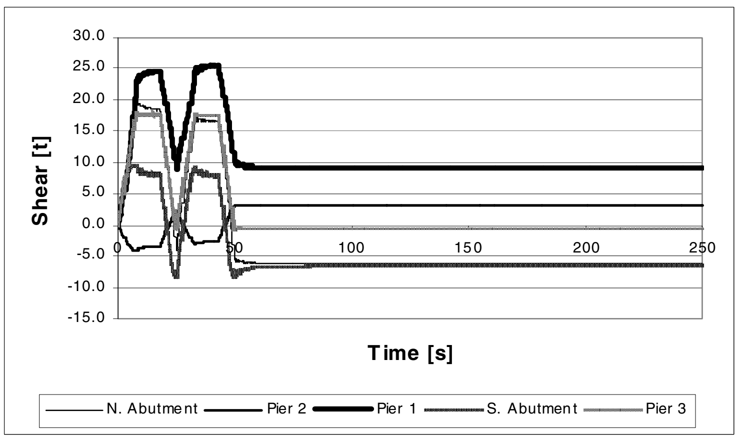


Coefficient of friction = 0.03

**Figure 7. Shear forces at top of piers due to wind.**

**Combined effect of wind and temperature.**

The temperature was measured with a continuous monitoring system in different sections of the bridge during several days. The location of sensors is described in figure 8, Riquelme [4]. A typical variation of temperature with time is in figure 9. It can be observed that the average temperature varies between 12 and 22 °C. The local peaks observed in sensors 1 and 6, which are located on the interior of the beam's steel walls, are due to the direct action of the sun rays. At the same time the relative displacements at sliding bearing were measured directly by LVDT sensors. Figure 10 shows the displacements obtained at the north abutment during September 29$^{th}$, 2003. The total displacement was near 18 mm. Because the system is non-linear, the effect of temperature and wind cannot be superimposed. A simultaneous analysis was then done using the SAP2000NL model. Figure 11 shows the displacements obtained for friction coefficients of 1 % and 3 % assuming a temperature increase of 6 °C, for 6 wind cycles, followed by a decrease of 12 °C and other 6 wind cycles. The maximum displacement obtained was 44 mm.

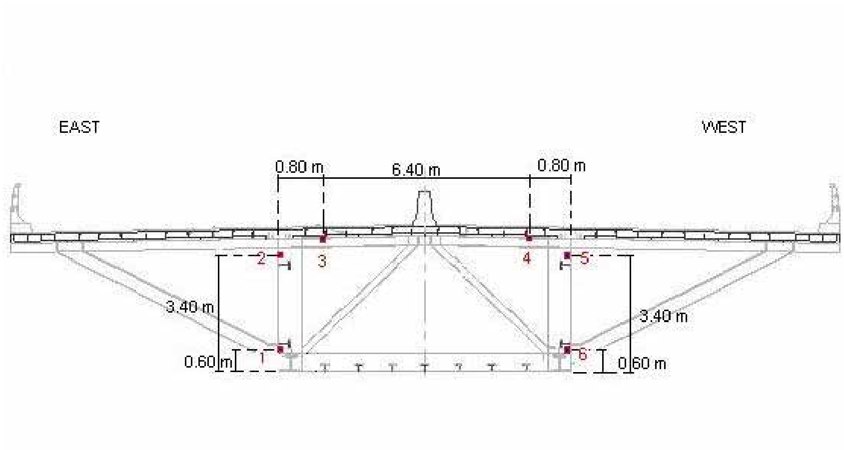


**Figure 8. Location of temperature sensors**

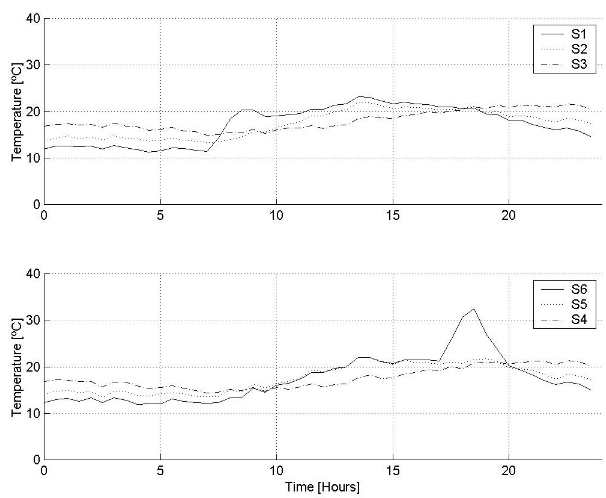


**Figure 9. Temperature variation at a given beam section.**

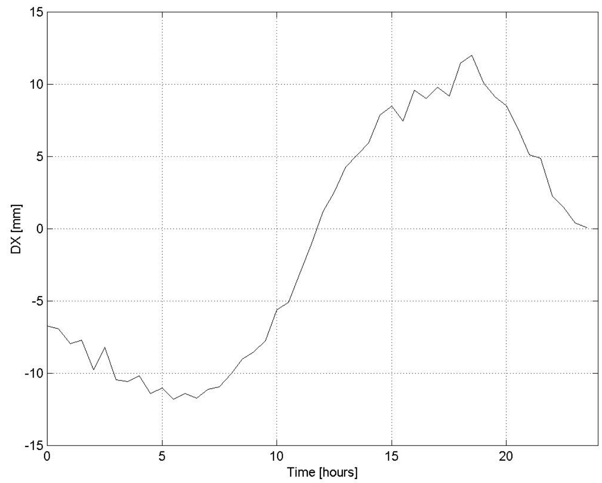


**Figure 10. Relative displacement at North abutment.**

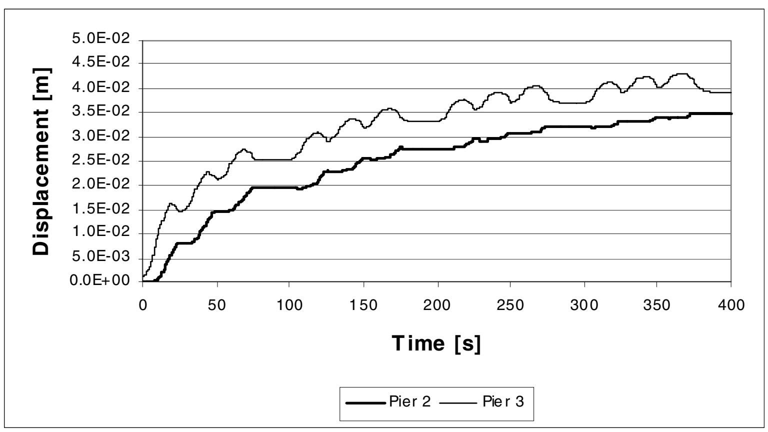


Coefficient of friction = 0.01

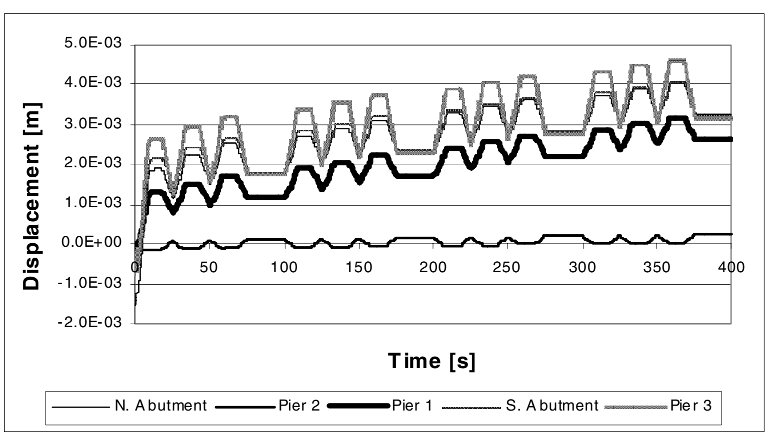


Coefficient of friction = 0.03

**Figure 11. Displacement due to combined wind and temperature.**

## CONCLUSION

The earthquake motions recorded at the Amolanas bridge show clearly the beneficial effects of base isolation and the nonlinear behavior caused by the action of the seismic isolation pads. The motion reduction is particularly significant in the longitudinal direction, in which the deck is free to move. It is smaller in the transverse direction, where stoppers limit the motion, and there is amplification in the vertical direction. The nonlinear behavior affects the instantaneous natural periods of the bridge that change with the level of excitation, and the values of damping that increase substantially in the first longitudinal mode (from 1.6 to 4.4 % from ambient vibrations to seismic action). The computer model developed to reproduce the response to ambient vibrations and to seismic excitation yields results generally in very good agreement with the recorded data, in spite of some minor discrepancies. The differences become more evident when looking at the Fourier spectra of the motions rather than their time histories. In relation to the wind and temperature effect on the bridge, it was concluded that for the maximum instantaneous wind velocity registered on site there be only negligible permanent displacements. However when the AASHTO design load was considered, a permanent displacement of as much as 44 mm was obtained, displacement that should be considered in the design of the isolation bearings.


## ACKNOWLEDGEMENTS

The authors wish to express their appreciation to the University of Chile for their financial support, to the Ministry of Public Works (Programa de Innovación Tecnológica) and to Fondecyt research fund (Projects Nº 1011025 and Nº 7011025). Most of the field and analytical work was carried out by graduate students Debora Riquelme and Elias Farias, supervised by instrumentation engineer Pedro Soto. Professor Ruben Boroschek made also valuable contributions in the analytical interpretation of field records.


## REFERENCES


1. Sarrazin, M., Moroni M., Boroschek R., and Tomaselli F. (2001) "Applications on seismic isolation and energy dissipation in bridges in Chile and Venezuela", *Proc. 7th International Seminar for Seismic Isolation, Passive Energy Dissipation and Active Control of Vibrations of Structures*, Assisi, Italy.
2. Tanaka, T., Yoshizawa, S., Osawa, Y., and Morishita, T., (1969). "Period and damping vibration in actual building modes", *Bull of Earthquake Research Institute*, 47, 1073-1092.
3. Farias, E. (2004). "Wind Effect on the Amolanas Bridge", *Civil Engineer Thesis,* University of Chile (in spanish).
4. Riquelme, D. (2004), "Temperature Effect on the Amolanas Bridge", *Civil Engineer Thesis,* University of Chile (in Spanish).